Surf. Sci. Letts., subm. 9/00

STM-induced Void Formation at the $Al_2O_3/Ni_3Al(111)$ Interface

N. P. Magtoto, C. Niu, M. Anzaldua and J. A. Kelber*
Department of Chemistry, University of North Texas, Denton, TX-76203
and
D. R. Jennison
Sandia National Laboratories, Albuquerque, NM 87185-1415

ABSTRACT

Under UHV conditions at 300 K, the applied electric field and/or resulting current from an STM tip creates nanoscale voids at the interface between an epitaxial, 7.0 Å thick Al_2O_3 film and a $Ni_3Al(111)$ substrate. This phenomenon is independent of tip polarity. Constant current (1 nA) images obtained at +0.1 V bias and +2.0 bias voltage (sample positive) reveal that voids are within the metal at the interface and, when small, are capped by the oxide film. Void size increases with time of exposure. The rate of void growth increases with applied bias/field and tunneling current, and increases significantly for field strengths >5 MV/cm, well below the dielectric breakdown threshold of 12 ± 1 MV/cm. Slower rates of void growth are, however, observed at lower applied field strengths. Continued growth of voids, to ~ 30 Å deep and ~ 500 Å wide, leads to the eventual failure of the oxide overlayer. Density Functional Theory calculations suggest a reduction-oxidation (REDOX) mechanism: interfacial metal atoms are oxidized via transport into the oxide, while oxide surface Al cations are reduced to admetal species which rapidly diffuse away. This is found to be exothermic in model calculations, regardless of the details of the oxide film structure; thus, the barriers to void formation

DISCLAIMER

DISCLAIMER

are kinetic rather than thermodynamic. We discuss our results in terms of mechanisms for the localized pitting corrosion of aluminum, as our results suggest nanovoid formation requires just electric field and current, which are ubiquitous in environmental conditions.

*Corresponding author, Ph: (940)-565-3265, FAX: (940)-369-8295, email: kelber@bob.unt.edu

Keywords: Scanning tunneling microscopy, density functional calculations, oxidation, corrosion, field effect, aluminum oxide, aluminum, nickel oxides, ceramic thin films, metal insulator interfaces.

In this Letter, we report nanovoid formation at the interface between a 7.0 Å thick Al_2O_3 film and a $Ni_3Al(111)$ substrate, caused by an STM tip under constant current feedback. First principles density functional theory (DFT) calculations suggest a facile local reduction-oxidation (REDOX) reaction, in which substrate metal is incorporated into the film and surface cations are reduced and diffuse away at room temperature.

The application of several volts across ultrathin (1-2 nm) films of dielectric materials can lead to extremely high electric fields and resulting tunneling currents. The behavior of ultrathin oxides under such conditions is of significant interest in microelectronics, because dielectric breakdown of the oxide has a direct impact on the stability of ultra-large scale integrated circuit devices [1] and the development of tunneling-based magnetoresistance devices [2, 3]. The effect of high electric fields on the stability of thin oxide films is also of critical importance in understanding possible connections between dielectric breakdown and the onset of localized corrosion (pitting) [4, 5]. The ability of STM to provide high spatial resolution and generate very high electric fields in a controlled ultrahigh vacuum (UHV) environment allows for the systematic assessment of the effects of electric fields on morphology, composition, and localized defect density (breakdown and pre-breakdown) at surfaces and interfaces.

The morphology and location of the STM-observed voids strongly resemble voids recently studied at the alumina/aluminum interface using positron annihilation spectroscopy [6], and also by atomic force microscopy during the dissolution of aluminum in aqueous NaOH [7]. In all cases, the nanovoids are in the metal itself and, when small, are capped by the oxide film overlayer. In the present work, however, no chemically corrosive agent is involved in the formation of interfacial voids.

The conditions which cause rapid nanovoid growth (fields ~ 5 MV/cm) are comparable to those generated at magnetoresistance junctions [8, 9] and also made by a halide ion adsorbed on the thin passivating oxide layer on aluminum metal in an aqueous environment [5]. Preliminary results at lower field strengths, however, indicate that void initiation and growth still occurs, but at rates difficult to observe.

Experiments were carried out in a UHV surface analysis system [10] (base pressure, 3×10^{-11} Torr) equipped with LEED, AES and STM. Al_2O_3 films were grown by directly oxidizing a clean $Ni_3Al(111)$ substrate at 300 K. The 7.0 ± 1 Å thick ordered Al_2O_3 was obtained by annealing at 1100 K, as described previously [10]. Recent studies [11, 12] have demonstrated that such oxide films are pure Al_2O_3, and that a (111)-oriented monolayer of metallic Al atoms exists at the $Al_2O_3/Ni_3Al(111)$ interface [10], just beneath a layer of chemisorbed oxygen – thus the actual Al_2O_3 material does not start until the second O-layer. The ordered Al_2O_3 film was stressed either by applying voltage pulses to the tip or holding the voltage constant at a given location on the surface for a specified time. (Application of a positive gap voltage to the sample denotes the tunneling of electrons from the occupied states of the tip to the unoccupied states of the sample.)

The constant current feedback loop was active during high field exposure in order to prevent tip-sample physical interaction.

Voids were created as follows. After imaging a large area of the sample at +0.1 V gap voltage and 1.0 nA feedback current, the tip was positioned at a specific location above the surface. With the feedback loop set at 1 nA, voltage pulses were applied. In a single pulse, the gap voltage was raised step-wise to a specified value (pulse height), then instantaneously decreased back to the normal tunneling voltage of 0.1 V. Each incremental step required about 200 μs. Since the pulse height was always divided into 200 steps, the whole procedure was completed in about 40 ms. The magnitude of the electric field (F) can be estimated by dividing the applied voltage (V) by the distance (d) between the Al_2O_3/Ni_3Al interface and the tungsten tip ($F = V/d$), where d is the sum of the tip-oxide surface distance and the oxide thickness (7 Å). The values of the tip-oxide surface distance (~40 – 43 Å) were estimated from the plots between the gap voltage and tip-sample separation (not shown). Electric field strengths under such conditions are calculated to be ~ 5 – 7 MV/cm, well below the STM-induced dielectric breakdown threshold of 12 ± MV/cm recently reported for such films under UHV conditions [13]. After each high field exposure, the surface was imaged under normal tunneling conditions (1 nA constant feedback current, +0.1 V bias voltage).

Void formation was marked by the appearance of a depression in the STM image. Fig. 1a displays voids created by voltage pulsing to 3.5 V at various locations at the surface. The voids at positions 1 and 2 were produced by 2 and 8 pulses, respectively (Fig. 1a). It is evident from the line profiles in Fig. 1b that the void in position 2 is ~2 Å deeper and ~350 Å wider across the rim than the void in position 1; thus, the size of the

void cross sectional area vs. electric field. Under these experimental conditions, the electric field varies approximately linearly with the applied gap voltage. The data in Fig. 3a indicate that the rate of void growth increases rapidly above ~5 MV/cm. The threshold for void growth suggested by the data in Fig. 3a may be more apparent than real, since voids can be created even at field strengths below 4 MV/cm provided the surface is exposed to a field for a very long time ($\geq$ 2700 sec). Experiments at constant voltage and varying feedback limit indicate that void growth rate also increases with tunneling current at a given applied voltage (Fig 3b), although the growth rate apparently approaches an asymptotic value at higher currents.

Upon reaching a certain size, the void may induce a failure of the oxide overlayer. This is shown in Fig. 4. The constant current image of the metal substrate (Fig. 4a) shows the presence of a void ~ 30 Å in depth and 500 Å wide. Subsequent imaging at 1.0 V gap voltage (Fig. 4b) also shows a gap in the oxide overlayer. This result indicates that continued exposure to high bias voltage causes the void to grow wider and deeper into the metal, eventually causing the (assumed) collapse of the oxide overlayer. This behavior was also observed in an aggressive aqueous environment where the oxide film suffered a local collapse once the void grew to a critical size [19], larger than here because of a thicker oxide layer.

The apparent lack of a discernable voltage threshold suggests the process is not stimulated by a specific electronic excitation. In addition, bias polarity-independence and current-dependence argue against field-assisted diffusion across the interface. Field induced vacancy diffusion from within the metal can be ruled out because the applied

field does not extend far into the conducting substrate. The migration of vacancies from within the oxide is similarly improbable because the oxide film is of high quality and the data clearly demonstrate void growth into the metal.

A possible explanation is localized heating due to inelastic electron-phonon scattering, enabling the system to overcome a kinetic barrier. This mechanism would show a current and field dependence of void growth rate, consistent with the data in Fig. 3. A similar mechanism was proposed for Si-H bond-breaking at Si surfaces [20], while electronically stimulated processes within SiO_2 films have a discernable threshold [21].

To help define a mechanism, we turn to *ab initio* theory. This work used DFT [22] and slab calculations. Because energetics are compared, we used the generalized gradient approximation (GGA) known as "PW91" [23], as implemented in the Vienna *Ab-Initio* Simulations Package (VASP) [24]. Ultrasoft Vanderbilt pseudopotentials [25] accurately removed the core electrons with a plane wave cutoff of only 270 eV. Geometric relaxation used a damped molecular dynamics algorithm until all forces were less than 0.05 eV/Å. The slab had five layers of aluminum metal, with the bottom two frozen at the bulk GGA lattice constant of 4.035 Å. Because of long-range electrostatic interactions, the periodic vacuum gap due to the plane-wave basis always exceeded 18 Å.

As a model for the real film on $Ni_3Al(111)$ (which cannot be directly studied because of lattice-mismatch relief by domain rotation [11]), computations were performed with three and four O-layer commensurate alumina systems on Al(111), all having chemisorbed oxygen at the interface. This interface, first proposed for ultrathin alumina films on metals made by high temperature annealing in oxygen rich conditions

[12], receives further support from our angle resolved XPS results together with those of others [26]: We find two types of oxygen (chemisorbed and oxidic) to be present.

Above the layer of chemisorbed oxygen, two different phases of alumina were explored. The first is motivated by the recent observation of θ-alumina on NiAl(100) by A. Stierle, et al. [27]. This structure, found using X-ray scattering, supported a computational result [12] predicting that the normal preference for octahedral site Al-ions is reversed at the interface; thus in this extreme model, all Al ions occupy tetrahedral sites. In the second model, we used the recently determined structure for the κ-phase [28], which has ¼ tetrahedral and ¾ octahedral site Al-ions. This structure is similar to a recent DFT structure for the second O-layer in ~ 5 Å films on close-packed surfaces [29], and is a more realistic model for the so-called [11] γ′ -films. We find that the qualitative results are *independent* of the details of oxide film structure.

In all cases it is found that the REDOX reaction (Fig. 5) is preferred energetically. In fact, for Al(111) with this interface, *the entire first layer of Al* prefers to be taken up into the oxide, even at the expense of becoming non-stoichiometric, with extra Al atoms reduced to adsorbed Al (Fig. 5). This movement is preferred by 0.15 (0.21) eV per Al atom in the tetrahedral (κ-phase) film. While these results agree with independent experimental observations of the alumina/aluminum system [26], that show a preference for the incorporation of chemisorbed oxygen into aluminum oxide islands, the results cannot be directly applied to the present case: starting with a perfect interface, the first REDOX reaction breaks 6 Al-Al and 3 Al-Ni bonds, vs. 9 Al-Al in the model systems. Given the melting temperatures of Al metal (660 C) and Ni_3Al (1390 C) vs. pure Ni (1455 C), Ni-Al bonds are much stronger than Al-Al, thus reducing the exothermicity.

However, these results are consistent with a kinetically limited REDOX mechanism, and one reason for the above energetics is the strong binding of Al adatoms to alumina [30].

Overall, the above results suggest nanovoid formation in the presence of electric field and induced current is a likely critical step in the corrosive pitting of aluminum (and possibly of other metals) and might significantly affect the durability of alumina-based tunneling junctions. Remaining to be addressed are the fundamental mechanisms of total mass transport (both interfacially and *within* the void) and whether only Al or both Al and Ni move across the interface. In addition, it is not known how formation and growth are related to the cohesive energy of the substrate material. However, with respect to the existing experimental and theoretical results, we make the following conjectures:

(1) *The presence of nanovoids at the alumina/aluminum (or aluminum alloy) interface is ubiquitous.* Voids are produced by non-uniform electric fields and currents in the passivating oxide layer; such occur in an electrochemical environment and are supported by the resulting oxide point defects [4,5]. The induced fields are similar in magnitude to those in the present study [5], while the metal cohesive energy is lower. This conjecture is also consistent with recent positron studies of alumina/aluminum interfaces [6] and with new experimental results indicating that Cl^- anions do not penetrate existing oxide films under open circuit conditions, even though pitting can occur under such conditions [31-33].

(2) *The transition from nanovoids to microscopic corrosion pits is induced by the collapse of, and/or the presence of microcracks in, the oxide,* when void growth causes local mechanical failure from factors such as strain. Cracks allow the transport of anionic species into the void, that grow into pits because metal is etched into soluble compounds.

Local fluid flow conditions, vs. the formation of insoluble scales and/or new oxide films at the pit surface, determine the balance between growth and passivation.

Acknowledgements

The authors gratefully acknowledge informative discussions with J. Sullivan, N. Missert, J. C. Barbour and K. Hebert. Work at UNT was supported in part by the U.S. DOE, Office of Basic Energy Sciences, under Grant No. DE-FG03-93ER45497, in part by the Robert Welch Foundation, under Grant No. B-1356, and in part by NSF, under Grant No. CHE-9714580, which are gratefully acknowledged. Sandia is a multi-program laboratory operated by Sandia Corporation, a Lockheed-Martin Company, for the U. S. DOE under Contract DE-AC04-94AL85000. This work was partially supported by a Laboratory Directed Research and Development Project and by the U. S. DOE Office of Basic Energy Sciences, Metals and Ceramics Division.

References

[1] J. F. Verwij and J. H. Klootwijk, Microelectronics Journal 27 (1996) 611.

[2] T. Miyazaki and N. Tezuka, J. Magn. Magn. Mater. 139 (1995) L231.

[3] B. G. Park and T. D. Lee, IEEE Trans. on Magnetics 35 (1999) 2919.

[4] J. P. Sullivan, J. C. Barbour, R. G. Dunn, K.-A. Son, L. P. Montes, N. Missert, and R.G. Copeland, in: *Critical Factors in Localized Corrosion III* (Electrochem. Soc. Proc.), Vol. 98-17, Eds. R. G. Kelly, P. M. Natishan, G. S. Frankel, and R. C. Newman, (Electrochemical Society, Inc., Pennington, New Jersey, 1998), p. 111.

[5] J. P. Sullivan, R. G. Dunn, J. C. Barbour, F. D. Wall, N. Missert, and R. G. Buchheit, in: *Oxide Films* (Electrochem. Soc. Proceed.), Vol. 2000-4, Eds. K. R. Hebert, R.

S. Lillard, and B. R. MacDougall, (Electrochemical Society, Inc., Pennington, NJ, 2000), in press.

[6] M. Formino, K. R. Hebert, P. Asoka-Kumar, and K. G. Lynn, Ibid. p. 642.

[7] K. R. Hebert, H. Wu, T. Gessmann, and K. Lynn, J. Electrochem. Soc., in press.

[8] W. Oepts, H. J. Verhagen, W. J. M. d. Jonge, and R. Coehoorn, Appl. Phys. Lett. 73 (1998) 2363.

[9] W. Oepts, H. J. Verhagen, R. Coehoorn, and W. J. M. d. Jonge, J. Appl. Phys. 86 (1999) 3863.

[10] S. G. Addepalli, B. Ekstrom, N. P. Magtoto, J. S. Lin, and J. A. Kelber, Surf. Sci. 442 (1999) 385.

[11] C. Becker, J. Kandler, H. Raaf, R. Linke, T. Pelster, M. Draeger, M. Tanemura, and K. Wandelt, J. Vac. Sci. and Technol. A16 (1998) 1000; A. Rosenhahn, J. Schneider, J. Kandler, C. Becker, and K. Wandelt, Surf. Sci. 433-435 (1999) 705.

[12] D. R. Jennison, C. Verdozzi, P. A. Schultz, and M. P. Sears, Phys. Rev. B59 (1999) R15605.

[13] N. P. Magtoto, C. Niu, B. Ekstrom, S. Addepalli and J. A. Kelber, Appl. Phys. Lett. (in press)

[14] P. Avouris and R. Wolkow, Appl. Phys. Lett. 55 (1989) 1074.

[15] T. Bertrams, A. Brodde, and H. Neddermeyer, J. Vac. Sci. Technol. B 12 (1994) 2122; see also M. Baumer and H.-J. Freund, Prog. in Surface Science, 61 (1999) 127.

[16] M. C. Gallagher, M. S. Fyfield, J. P. Cowin, and S. A. Joyce, Surf. Sci. 339 (1995) L909.

[17] K. Fujita, H. Watanabe, and M. Ichikawa, J. Appl. Phys. 83 (1998) 3639.

[18] A. Rosenhahn, J. Schneider, J. Kandler, C. Becker, and K. Wandelt, Surf. Sci. 433 (1999) 705.

[19] The critical void size for oxide collapse was much larger than observed here, but the oxide film was also much thicker. L. F. Lin, C. Y. Chao, and D. D. MacDonald, J. Electrochem. Soc. 128 (1981) 1194.

[20] H. C. Akpati, P. Nordlander, L. Lou and Ph. Avouris, Surface Science 372 (1997) 9.

[21] D. R. Jennison, J. P. Sullivan, P. A. Schultz, M. P. Sears and E. B. Stechel, Surface Science 390 (1997) 112.

[22] P. Hohenberg and W. Kohn, Phys. Rev. 136 (1964) B864; W. Kohn and L. J. Sham, Phys. Rev. 140 (1965) A1133.

[23] J. P. Perdew, J. A. Chevary, S. H. Vosko, K. A. Jackson, M. R. Pederson, D. J. Singh, C. Fiolhais, Phys. Rev. B 46 (1992) 6671.

[24] G. Kresse and J. Hafner, Phys. Rev. B 47 (1993) 558; 49 (1994) 14251; 54 (1996) 11169.

[25] D. Vanderbilt, Phys. Rev. B 32 (1985) 8412; 41 (1990) 7892.

[26] I. Popova, V. Zhukov, and J. T. Yates, Jr., J. Appl. Phys. 87, 8143 (2000).

[27] A. Stierle, V. Formoso, F. Comin, and R. Franchy, Surf. Sci., in press.

[28] Y. Yourdshahyan, C. Ruberto, M. Halvarsson, L. Bengtsson, V. Langer, B. I. Lundqvist, S. Ruppi, U. Rolander, J. Amer. Ceramic Soc. 82 (1999) 1365.

[29] D. R. Jennison and A. Bogicevic, Surf. Sci., in press.

[30] A. Bogicevic and D. R. Jennison, Phys. Rev. Letts. 82 (1999) 4050.

[31] Y. Xu, M. Wang, and H. W. Pickering, J. Electrochem. Soc. 140 (1993) 3448.

[32] P. Marcus and J.-M. Herbelin, Corrosion Science 34 (1993) 1123

[33] Bruce Bunker, unpublished results.

Figure Captions:

Fig. 1. (a) STM constant current (0.1 nA, 0.1 V bias) images of pits formed into a "U" with varied numbers of pulses to (see text) +3.5 V (sample positive) bias. The substrate is a 7.0 Å thick Al_2O_3 film on a $Ni_3Al(111)$ substrate. (b) Cross sectional line scans of different regions of the "U" after application of 2 and 8 pulses to 3.5 V, respectively.

Fig. 2. STM constant current (1 nA) images of a region of the $Al_2O_3/Ni_3Al(111)$ film after 30 pulses to 3.5 volts. (a) Image acquired at 0.1 V bias, with tunneling between tip and metal states; (b) Image of the same region acquired at 2.0 V bias, with tunneling between tip and oxide states.

Fig. 3. (Top) Void cross sectional area after 300 sec exposure vs. the electric field strength . (Bottom)Void cross sectional area , after 300 sec exposure, vs tunneling current.

Fig. 4. STM constant current images showing a large void and collapse of the oxide overlayer. (a) Constant current image (1nA, 0.1V bias) showing the void present at the oxide/metal interface; (b) Constant current image (1nA, 1.0 V bias) of the same region showing a gap (presumed collapse) in the oxide overlayer.

Fig. 5. Schematic diagram indicating the proposed REDOX mechanism. Atoms are oxygen in white, Al metal in gray, Al ions in black. After the first atom goes, it is easier for the next because of reduced coordination. The reduced Al adatom height is shown.

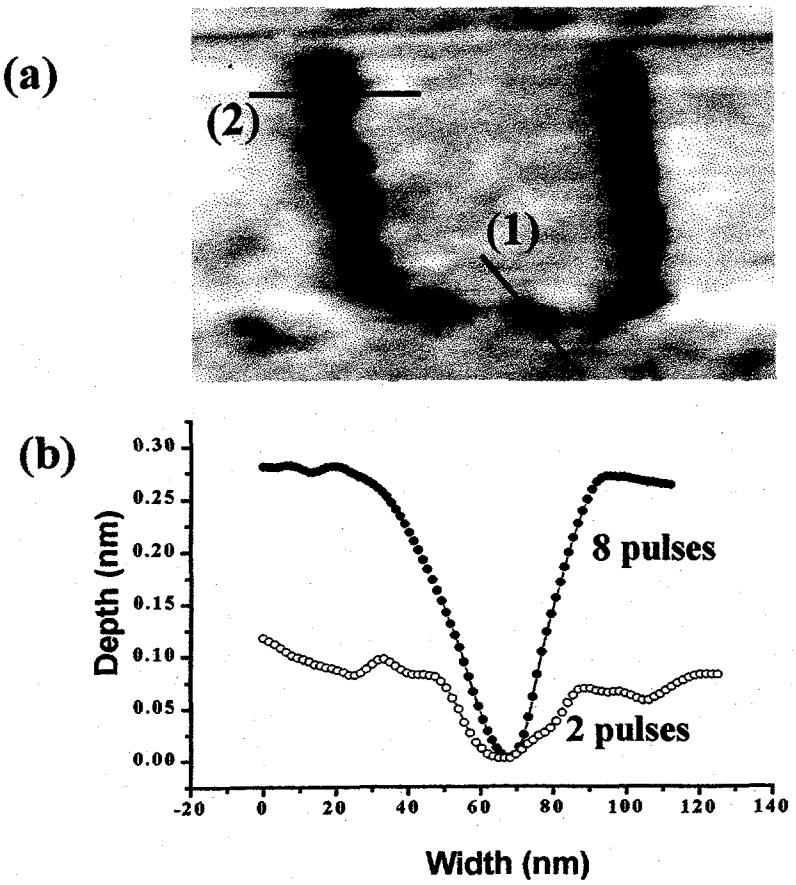

Fig. 1 Magtoto et al., STM-induced Void Formation

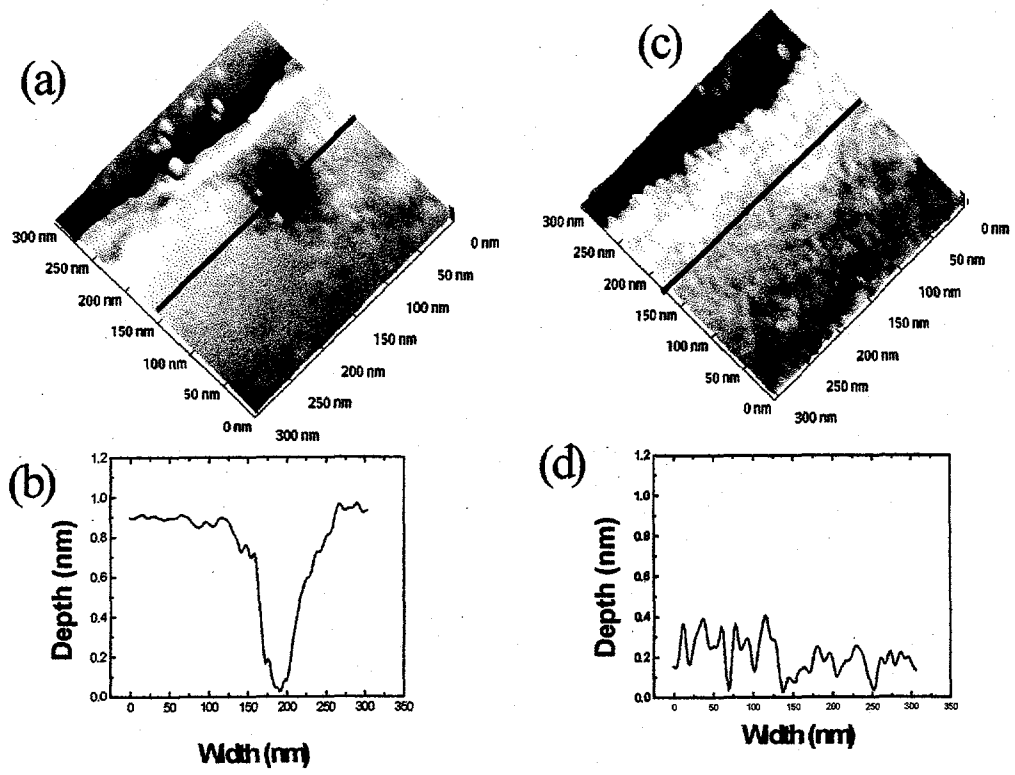

Fig. 2 Magtoto et al., STM-induced Void Formation

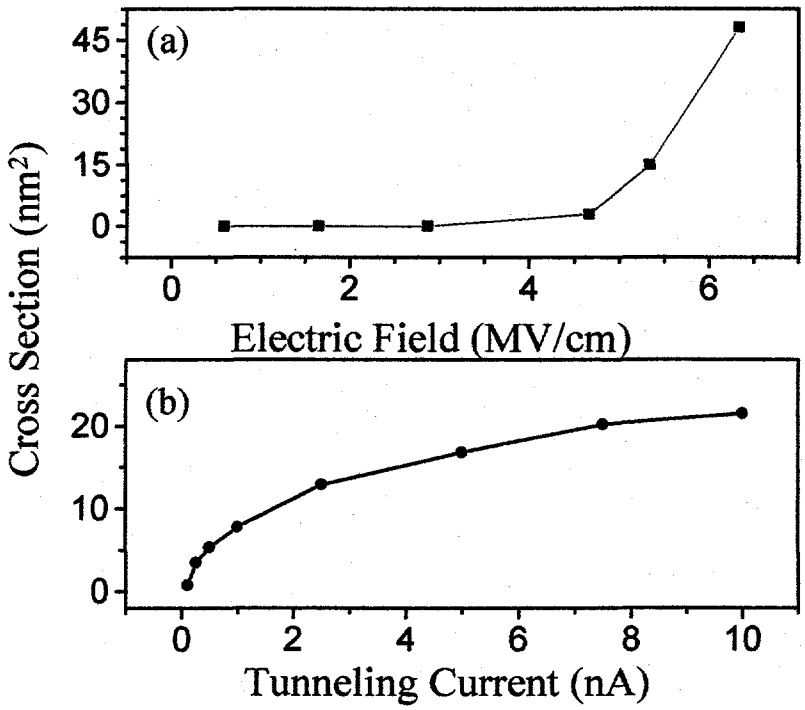

Fig. 3 Magtoto et al., STM-induced Void Formation

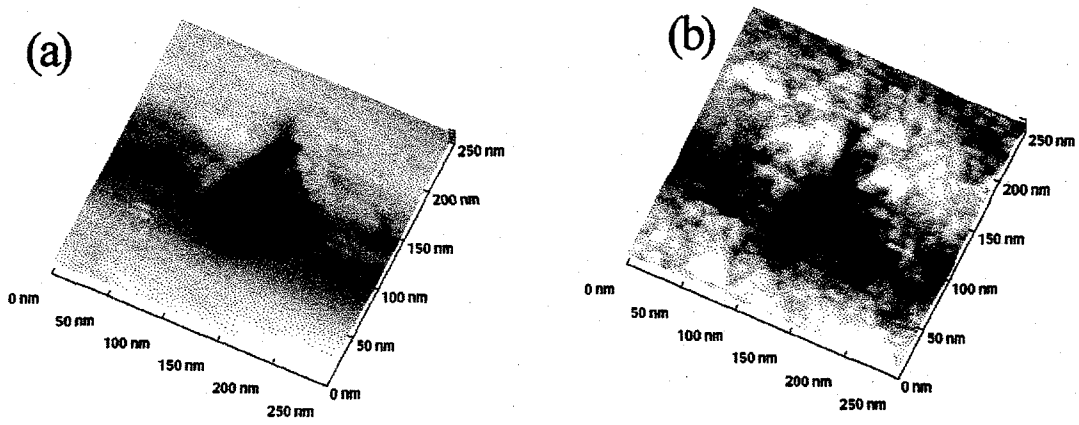

Fig. 4 Magtoto et al., STM-induced Void Formation

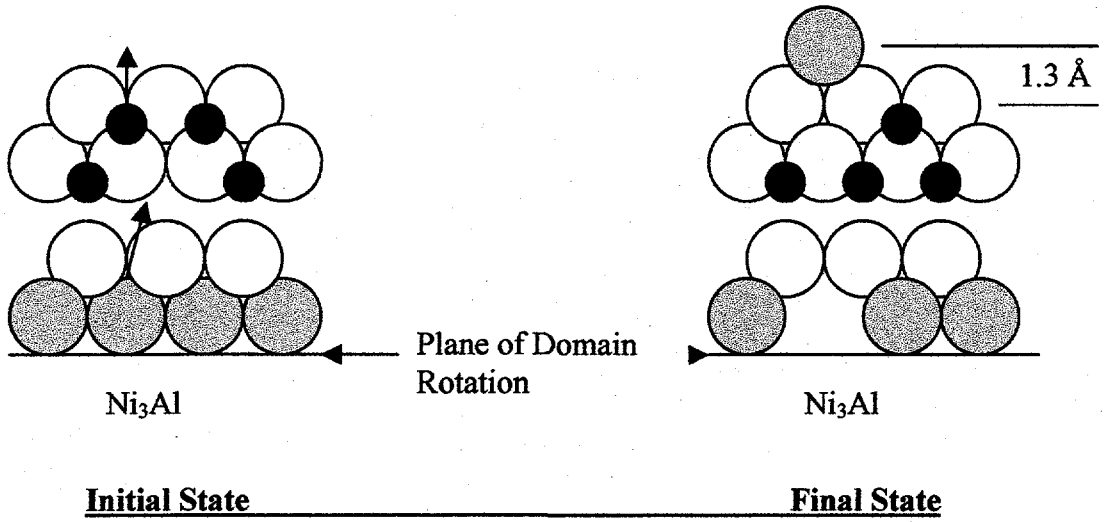

Figure 5 – Magtoto et al., STM-induced void formation...